2003

Heterogeneous electron-transfer kinetics with synchrotron 57Fe Mossbauer spectroscopy

J. E. Amonette
Pacific Northwest National Laboratory, jim.amonette@pnl.gov

Ravi K. Kukkadapu
Pacific Northwest National Laboratory, ravi.kukkadapu@pnl.gov

E. E. Alp
Argonne National Laboratory

W. Sturhahn
Argonne National Laboratory

T. S. Toellner
Argonne National Laboratory

Pergamon

Geochimica et Cosmochimica Acta, Vol. 67, No. 12, pp. 2109–2116, 2003

0016-7037/03 $30.00 + .00

doi:10.1016/S0016-7037(00)01346-7

Heterogeneous electron-transfer kinetics with synchrotron ^{57}Fe Mössbauer spectroscopy

J. E. Amonette,[1,*] R. K. Kukkadapu,[1] E. E. Alp,[2] W. Sturhahn,[2] and T. S. Toellner[2]

[1]Environmental Molecular Sciences Laboratory, Pacific Northwest National Laboratory, Richland, WA 99352, USA
[2]Advanced Photon Source, Argonne National Laboratory, Argonne, IL 60439, USA

(*Received March* 1, 2002; *accepted in revised form October* 31, 2002)

Abstract—In the first known kinetic application of the technique, synchrotron ^{57}Fe-Mössbauer spectroscopy was used to follow the rate of heterogeneous electron transfer between aqueous reagents and a solid phase containing Fe. The solid, a synthetic ^{57}Fe-enriched Fe(III)-bearing pyroaurite-like phase having terephthalate (TA) in the interlayer [$Mg_3Fe(OH)_8(TA)_{0.5} \cdot 2H_2O$], was reduced by $Na_2S_2O_4$ and then reoxidized by $K_2Cr_2O_7$ by means of a novel flow-through cell. Synchrotron Mössbauer spectra were collected in the time domain at 30-s intervals. Integration of the intensity obtained during a selected time interval in the spectra allowed sensitive determination of Fe(II) content as a function of reaction time. Analysis of reaction end member specimens by both the synchrotron technique and conventional Mössbauer spectroscopy yielded comparable values for Mössbauer parameters such as center shift and Fe(II)/Fe(III) area ratios. Slight differences in quadrupole splitting values were observed, however. A reactive diffusion model was developed that fit the experimental Fe(II) kinetic data well and allowed the extraction of second-order rate constants for each reaction. Thus, in addition to rapidly collecting high quality Mössbauer data, the synchrotron technique seems well suited for aqueous rate experiments as a result of the penetrating power of 14.4 keV X-rays and high sensitivity to Fe valence state.

1. INTRODUCTION

Through a combination of its abundance and a range in reduction potentials for the common Fe(II)/Fe(III) couple that spans the aqueous regime, iron (Fe) asserts a dominant role in the aqueous chemistry of natural systems ranging from soils and ocean sediments to living cells and higher organisms. In each of these systems, the rate of the Fe redox transformation, and in particular, the structural changes that occur during the transformation, are of primary importance in understanding the chemistry (Amonette, 2003). Conventional experimental techniques for measuring these parameters, however, have been limited to static approaches in which initial and final states are determined (e.g., conventional Mössbauer spectroscopy), or to approaches where magnetic interactions in high-Fe solids diminish signal quality (e.g., electron paramagnetic spectroscopy). The recent development of third-generation synchrotron radiation sources, however, has made possible the application of techniques such as X-ray near-edge structure (XANES) spectroscopy (Bajt et al., 1994; Delaney et al., 1998; Dyar et al., 1998; Schmuki et al., 1998) and synchrotron Mössbauer spectroscopy to this class of problems.

Synchrotron Mössbauer spectroscopy, otherwise known as coherent forward nuclear resonance scattering, shows great potential for kinetic studies of Fe systems. It has an inherently large signal-to-noise ratio as a result of the collection of data in the time regime rather than the energy regime and can yield the same parameters as obtained by conventional Mössbauer spectroscopy (Alp et al., 1995, 2001a,b; Sturhahn et al., 1998). This technique has recently become practical through the coupling of high-brilliance undulator insertion devices with high-resolution monochromators (Toellner et al., 1997; Alp et al., 2001a) that allow photons having fluxes of 10^8 s^{-1} and spectral bandwidths of less than 1 meV to be focused on the sample. Here we report the first such use of SMS to monitor the rate of a heterogeneous reaction involving the reduction and reoxidation of Fe in a model ^{57}Fe-enriched pyroaurite-like compound.

* Author to whom correspondence should be addressed (jim.amonette@pnl.gov).

2. MATERIALS AND EXPERIMENTAL METHODS

2.1. Fe-Bearing Mineral

An Fe(III)-bearing pyroaurite-like compound having terephthalate in the interlayer [$Mg_3Fe(OH)_8(TA)_{0.5} \cdot 2H_2O$, where TA refers to terephthalate] was selected for the solid-phase reactant. This claylike compound is a member of the broad class of compounds known as layered hydroxides or anionic clays. Other members of this class include the hydrotalcite minerals, and the green rusts, which have been implicated as key reductants in the nitrogen cycle (Hansen and Koch, 1998; Hansen et al., 2001). The structure of layered hydroxides, which is similar in some respects to that of brucite [$Mg(OH)_2$], consists of 0.48-nm thick layers of edge-sharing $M(OH)_6$ octahedra separated by an interlayer region and, in general, is stable for M(II):M(III) ratios of between 1 and 8 (Miyata et al., 1975; Miyata, 1975; Drezdzon, 1988). In our compound (Fig. 1), substitution of Fe(III) for Mg(II) in the structure generates a positive charge in the layer that is balanced by TA anions located in the interlayer region along with water molecules. Local ordering of the Fe(III) cations is expected (Vucelic et al., 1997) such that no pairs of Fe(III) ions occupy adjacent octahedral sites, which otherwise are structurally equivalent. The orientation of the C-COO^- axis of the terephthalate anions is perpendicular to the hydroxide layer (Maxwell et al., 1999) giving rise to an open gallery (~0.94 nm) between the hydroxide layers and ready access of water and dissolved reagents to the internal surfaces of the hydroxide layers. As a result of these structural properties, the compound was expected to exhibit rapid electron-transfer kinetics when exposed to an aqueous reagent.

To ensure an adequate signal and a correspondingly high time resolution, we prepared specimens that were enriched in ^{57}Fe. We obtained 400 mg of Fe(m) enriched to 92.4% with the ^{57}Fe isotope (Isotec, Inc., Miamisburg, OH), dissolved it in hot 48% HNO_3, and then crystallized the $Fe(NO_3)_3$ hydrate by chilling to 4°C. This salt was then used with $Mg(NO_3)_2 \cdot 6H_2O$, $Al(NO_3)_3 \cdot 9H_2O$, NaOH, and Na-terephthalate to synthesize a pyroaurite-like compound with a

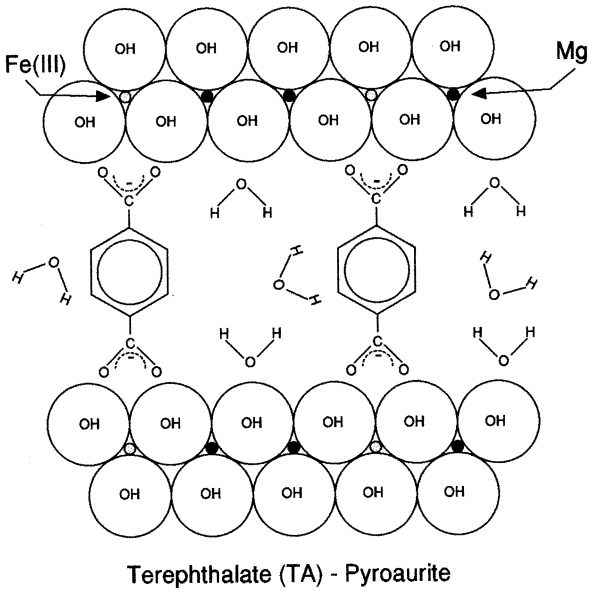

Fig. 1. Schematic (scale approximate) of pyroaurite-like compound with terephthalate (TA) anions and water molecules in the interlayer. Cross section is normal to plane of hydroxyl layers.

Mg:Fe ratio of 3 following the method of Kukkadapu et al. (1997). Compounds prepared at pH 10 and 8.5 were used interchangeably in the experiments as their layer charge and other properties are essentially the same (Kukkadapu et al., 1997).

2.2. Reaction Apparatus

A novel flow-through cell, consisting of a specimen holder inserted into a reaction vessel, was constructed from polyetheretherketone to allow collection of Mössbauer spectra during the course of the reaction (Fig. 2). The specimen holder contained the powdered specimen (~9 mg) in the form of a thin disk 6 mm in diameter and 500 μm thick. Polycarbonate filter membranes (13 mm diameter, 25 μm thick, 0.2 μm pores, Osmonics, Livermore, CA) formed the ends of the disk, thus retaining the powder and allowing the reacting solution to diffuse into the specimen. The specimen holder was mounted inside the reaction vessel and bathed in the reacting solution, which entered and left the vessel through four ports connected to supply and receiving reservoirs with standard liquid-chromatography hardware. Optical access to the reaction chamber and specimen holder was provided by means of a 6-mm-diameter optical tunnel aligned with the incident X-ray beam and sealed by four thin polymer-film windows to retain the fluid and prevent interactions with atmospheric constituents. Details of the design may be obtained from the corresponding author.

2.3. Synchrotron Mössbauer Experiments

Experiments were conducted at the Advanced Photon Source (Argonne, IL) on beamline 3-ID-B operated by the Synchrotron Radiation Instrumentation Collaborative Access Team (SRI-CAT). Monochromatic synchrotron radiation centered at the ^{57}Fe Mössbauer resonance near 14.41 keV and having a band pass of approximately 0.6 meV was provided by two sets of Si-crystal double monochromators (Toellner et al., 1997). The beam was rectangular in cross section with dimensions of 3 mm horizontally and 1 mm vertically. During the runs (September 1997; February 1998) the synchrotron was operated in singlet filling mode with bunches spaced every 150 ns. The intensity of the forward-scattered resonant light was detected in time after each bunch passed through the undulator.

The reducing solutions consisted of $Na_2S_2O_4$ freshly prepared in Na_2TA, which buffered the solutions at pH ~5. In the September 1997 synchrotron experiment, a 0.04 mol/L $Na_2S_2O_4$-0.16 mol/L Na_2TA solution was used. In the February 1998 synchrotron run and in the experiment that prepared a reduced specimen for conventional Mössbauer analysis, 0.05 mol/L $Na_2S_2O_4$-0.05 mol/L Na_2TA solutions were used. The oxidizing solution used in all experiments consisted of 0.05 mol/L $K_2Cr_2O_7$-0.05 mol/L Na_2TA that was 0.1 mol/L in Cr(VI). The reducing and oxidizing solutions were loaded into glass-walled syringes and metered through the reaction vessel at a rate of 0.25 mL min^{-1}. Time-domain spectra (i.e., "resonance relaxation" spectra) were accumulated for 30 s and stored before starting the next accumulation period.

A typical experiment consisted of the following steps. The sample was loaded into the flow-through cell, placed into the beam path, and the monochromator tuned to obtain the resonance energy. Deionized water was pumped through the cell at 0.25 mL min^{-1} with a syringe pump, and a few baseline spectra were collected. Then, the pumping fluid was changed to the $S_2O_4^{2-}$/TA solution and the repetitive collection of time-domain spectra was initiated with accumulation times of 30 s. Once the reduction reaction reached completion, as judged by no further change in successive spectra, collection of spectra ceased. The fluid in the syringe pump was changed back to deionized (DI) water for 15 to 30 min to purge the cell of the reductant that had not diffused into the specimen holder. To reoxidize the sample, the fluid was changed to the Cr(VI)/TA solution and collection of spectra resumed until reoxi-

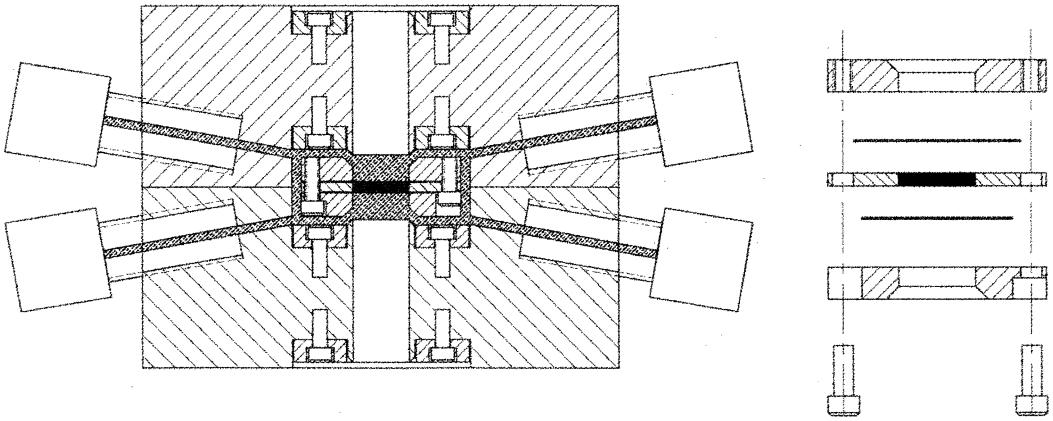

Fig. 2. Cross-sectional view of flow-through cell (left) and cylindrical specimen holder (right). Contact between specimen (solid black) and reactants (dense cross-hatching) is by diffusion of reactants through membranes at top and bottom of specimen holder. Monochromatic synchrotron light (14.414 keV) enters the cell and passes through the sample via the central tunnel.

dation was complete. The cell was then flushed again with DI water to remove remaining oxidant external to the specimen holder.

The synchrotron data were analyzed by CONUSS© software (Sturhahn, 1996). This program package performs nuclear resonant scattering calculations, compares them to the experimental results, and yields the usual Mössbauer spectroscopy output parameters such as center shift and quadrupole splitting.

2.4. Conventional Mössbauer Experiments

Essentially the same reaction procedure as used in the synchrotron experiments was used to prepare a reduced specimen for conventional Mössbauer analysis. After treatment for the same length of time as in the synchrotron experiments, the reaction cell was transferred to an anoxic chamber where the specimen holder was removed, and the specimen allowed to dry under N_2(g). The reoxidized specimen from the February 1998 synchrotron run was also analyzed by the conventional Mössbauer approach after drying under N_2(g).

For analyses of the reduced and reoxidized specimens, randomly orientated absorbers were prepared by mixing the entire dried specimen with petroleum jelly in a 6.35-mm-deep, 12.7-mm-diameter Cu(m) cylinder sealed at one end with clear Scotch tape. The holder was entirely filled with the petroleum jelly/specimen mixture (no bubbles were present) and then sealed at the other end with scotch tape. Spectra were collected at room temperature (RT) using an ~50 mCi (1.85 GBq) ^{57}Co/Rh single-line thin source mounted on an MVT-1000 (WissEL) velocity transducer operated in constant acceleration mode (23 Hz, $\pm$ 4 mm s^{-1}). An Ar-Kr energy-proportional counter was used to detect the radiation transmitted through the holder, and the counts detected were stored as a function of energy (transducer velocity) with a 1024-channel analyzer. Data were then folded to 512 channels to give a flat background. The zero-velocity position was calibrated at RT by an α-Fe(m) foil (20 μm thick) placed in exactly the same position as the specimen. Spectral analysis was performed with the Recoil program (University of Ottawa, Canada) using the Lorentzian method and no corrections for sample thickness.

2.5. Reactive Diffusion Model

A reactive two-front diffusion model was constructed to simulate the reaction progress inside the cell and allow the extraction of rate constants for the reduction and oxidation reactions. This model was based on a two-front model for simple diffusion into a slab (Jost, 1960, pp. 32–45), and was adapted to include the effects of reaction between the diffusing species and the solid-phase (Danckwerts, 1950, 1951). Two diffusion zones were assumed: first, a nonreactive zone consisting of the membrane on the outside of the specimen holder, and second, a reactive zone within the specimen holder that used a single diffusion coefficient to describe diffusion between particles, as well as that occurring within the interlayer galleries of those particles to the reaction front. A second-order rate law, which was first order in both the aqueous reagent and the solid-phase Fe, was assumed. The reactive surface area for the solid-phase Fe was modeled by assuming a radially retreating reaction front from the periphery of a cylindrical particle into the interior, as might be expected for a reaction occurring in the interlayer gallery of a disk-shaped pyroaurite-like compound (Koch, 1998). Thus, as the reaction progressed, the available surface for reaction decreased. Although diffusion of the aqueous reactants was being modeled, the desired output was in terms of the mole fraction of Fe(II) or Fe(III) in the solid (depending on the reaction) because this value corresponded to that measured spectroscopically.

Mathematically, the quantity of solid-phase Fe(II) [or Fe(III)] generated by reaction with $S_2O_4^{2-}$ (or $Cr_2O_7^{2-}$) at any point in time after contact of the reacting solution with the reaction cell was given by

$$Q_{Fe(t)} = (8/\pi)VmC_s[1 - \mathrm{erf}(b/\sqrt{(4D_1t)}] \sum_{n=0\to\infty}[1/(2n+1)]^2[(k + D_2W_n\exp(-kt - D_2W_nt)/(k + D_2W_n)) - \exp(-D_2W_nt)], \quad (1)$$

where V is the volume of the specimen, m is a factor to account for the stoichiometry of the reaction with Fe, C_s is the concentration of reagent in the bulk solution bathing the outside of the membrane, erf is the error function (Lasaga, 1998, p. 370), b is the thickness of the membrane, D_1 is the diffusion coefficient in the membrane, t is the contact time of reagent with the membrane, n is an integer, k is the pseudo-first-order rate constant for the reaction in terms of the soluble reagent, D_2 is the diffusion coefficient inside the specimen holder, and

$$W_n = [(2n + 1)(\pi/2P)]^2, \quad (2)$$

where 2P is the thickness of the specimen along the cylinder axis.

The pseudo-first-order rate constant

$$k = k_2S_{(0)}[1 - \alpha]^{1/2}[(Q_{Fe[un(0)]} - Q_{Fe(t)})/V], \quad (3)$$

where k_2 is the second-order rate constant, $S_{(0)}$ is the initial reactive surface area, α (the reaction coordinate) is equal to $Q_{Fe(t)}/Q_{Fe((\infty))}$, and $Q_{Fe[un(0)]}$ is the initial quantity of unreacted solid-phase Fe.

The model was implemented in a spreadsheet and parameterized manually until the best fit to the experimental data was obtained as determined by a least squares procedure. The variable parameters in the fitting procedure were C_s, D_1, D_2, and k_2. It was necessary to include C_s as a parameter to account for the strong attraction of the anionic reagents to the positively charged layers in the pyroaurite-like material. The infinite series in Eqn. 1 was truncated to the first 21 terms, after determination that the error associated with truncation was negligible, and values for erf were estimated as described by Lasaga (1998, p. 370). The pseudo-first-order rate constant k was evaluated for each time step using the average value for $Q_{Fe(t)}$ from the previous 10 time steps, and setting $S_{(0)}$ equal to 1. Reported values for k_2 thus include $S_{(0)}$ as a factor of unknown magnitude. A full derivation of the model is given in the Electronic Supplement.

3. RESULTS AND DISCUSSION

3.1. Mössbauer Spectra

The typical synchrotron Mössbauer spectrum is obtained in the form of intensity of the nuclear decay as a function of the time after each light pulse strikes the specimen. In the absence of resonance, the entire pulse passes through the sample at t = 0. This light yields a prompt signal that decays with the detector fall time. When nuclear resonance is excited, however, the absorbed light is reemitted, the time-resolved intensity of which contains information about the sample (Fig. 3). The relative shapes of the peaks and the positions of the valleys (i.e., nodes) between them contain information about the electronic and structural environment of the resonating atoms. The resulting time spectrum is a Fourier transform of the energy spectrum, and it can be simulated with coherent forward scattering formalism developed into a computer code, CONUSS© (Sturhahn, 1996).

Ten-minute spectra for untreated (oxidized) specimens and for specimens reduced to the maximum extent of the treatment, clearly show differences in the spacing of the nodes, with the reduced spectra having more closely spaced nodes, indicative of larger average quadrupole-splitting values (Fig. 3). Under the conditions of this experiment, it was possible to collect data for as short a period as 30 s and still have enough signal to determine the location and shape of the peaks and nodes (Fig. 3), inset). By selecting a portion of the time spectrum exhibiting the greatest signal contrast between oxidized and reduced spectra, and integrating the signal obtained in this window, a very sensitive measure of reaction progress was obtained. Thus, for the spectra shown in Figure 3, the signal from a window set between 22 and 40 ns can be used to follow the kinetics of the reaction at time steps as small as 30 s.

Conventional Mössbauer spectra collected for the untreated (oxidized), reduced, and reoxidized specimens (Fig. 4) show

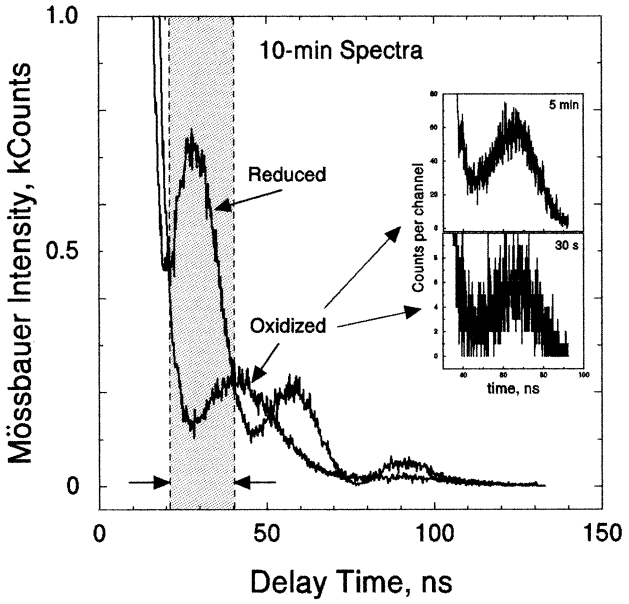

Fig. 3. Typical synchrotron spectra for oxidized and reduced samples (September 1997 run), with region showing time window for integration if only rate information needed and inset showing ultimate time resolutions (i.e., 5-min and 30-s spectra).

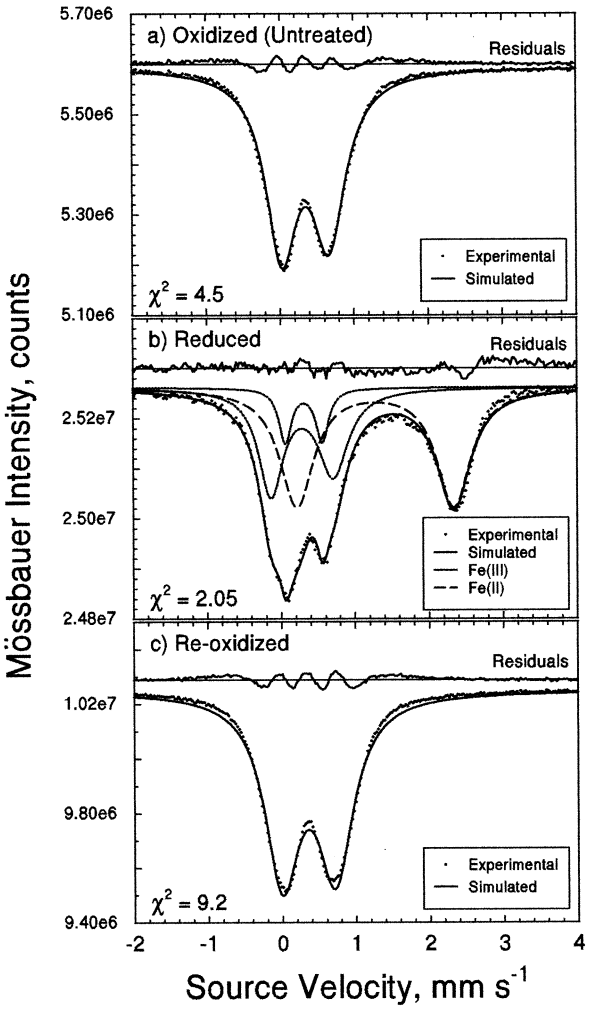

Fig. 4. Conventional Mössbauer spectra for untreated (oxidized), reduced, and reoxidized specimens.

the near complete reversibility of the reaction, with the only apparent change between untreated and reoxidized spectra being a slight broadening of the Fe(III) doublet. Magnetic hyperfine interactions are absent from all three spectra, and the development of a strong Fe(II) doublet with reduction is consistent with expectations for pyroaurite-like compounds (Raki et al., 1995). The Fe(III) contribution to the reduced spectrum (Fig. 4b) was fit with two doublets, indicating a considerable broadening in the range of possible Fe(III) environments as a result of reduction of some of the neighboring Fe(III) atoms to Fe(II). The slight asymmetry of the Fe(III) doublets in all three spectra (1.04 to 1.10) is not likely a result of texture effects as these are eliminated by the specimen-preparation technique used (Rancourt, 1994), and may therefore be a manifestation of the Goldanskii-Karyagin effect (Raki et al., 1995; D. G. Rancourt, personal communication). An alternative explanation is that a distribution of Fe(III) sites in the mineral (i.e., cation disorder) gives rise to the asymmetry observed (Koch, 1998).

Comparison of the Mössbauer parameters derived from parallel conventional and synchrotron analyses of untreated (oxidized) and maximally reduced specimens (Table 1) show very good agreement in terms of center shift and relative peak areas assigned to Fe(II) and Fe(III). Some differences exist in the determinations of quadrupole-splitting values, however. Slight increases in the center-shift and quadrupole-splitting values are seen between the untreated (oxidized) and reoxidized samples with conventional analysis. By using a single doublet, the quality of the fit was significantly poorer for the reoxidized sample (χ^2 = 9.20) than for the untreated (oxidized) sample (χ^2 = 4.54), suggesting an increase in the diversity of Fe(III) sites as a result of the treatments. Koch (1998) obtained the best fits to oxidized pyroaurite specimens by using a quadrupole-splitting-distribution (QSD) approach rather than the Lorentzian approach taken here. Indeed, when we fit the reduced spectrum using the QSD approach, a better fit was obtained, but the Fe(II)/Fe(III) ratio was the same as obtained with the simpler Lorentzian model. Because our primary concern was with the Fe(II)/Fe(III) ratio, we used the simpler Lorentzian model for all spectra.

The reaction did not proceed to complete reduction of the structural Fe(III) (Table 1). At the maximum of 55 to 58% reduction, the M(II):M(III) ratio in our compound was ~7.9 to 8.5, close to the maximum ratio of 8 observed in layered-hydroxide synthesis experiments by Miyata et al. (1975). Given the known chemical stability of brucite and amakinite [$Fe(OH)_2$], which have no interlayer gallery, it is unlikely that complete destruction of the compound occurs at higher Fe(II) content. Rather, we suspect that at higher levels of reduction (i.e., larger M(II):M(III) ratios) the layer charge (and hence the quantity of TA propping the layers apart) decreases sufficiently that a collapse of the interlayer region occurs. With such a collapse, further access of reductant to most of the structural Fe(III) is prevented and reduction ceases. Similar reaction-limiting processes involving access to the interlayer region

Table 1. Mössbauer parameters obtained by conventional and synchrotron (September 1997 run) spectroscopic approaches for untreated (oxidized) and maximally reduced specimens, and by the conventional approach for a reoxidized specimen.

			Mössbauer parameters			
Sample	Site	Technique	CS[a] (mm s^{-1})	QS[b] (mm s^{-1})	Area (%)	χ^2
Untreated (Oxidized)						
	Fe(III)	Conventional	0.34	0.64	100	4.54
		Synchrotron	0.31	0.57	100	4.60
Reduced						
	Fe(III)	Conventional	0.31	0.50	9.4 } 44	2.05
			0.29	0.84	35	
		Synchrotron	0.31	0.60	42	7.90
	Fe(II)	Conventional	1.27	2.12	55	2.05
		Synchrotron	1.23	2.42	58	7.90
Reoxidized						
	Fe(III)	Conventional	0.36	0.72	100	9.20
		Synchrotron	—	—	—	—

[a] Center shift
[b] Quadrupole splitting

have been observed for the oxidation of Fe(II) in biotites (Scott and Amonette, 1988; Amonette and Scott, 1995).

The synchrotron spectra for 10 successive 30-s time steps during the course of the reduction and reoxidation reactions were summed to yield 5-min spectra. A representative series of these summed spectra from each reaction was selected and plotted in stacked mode to show the qualitative changes occurring during the reactions (Fig. 5). The main changes observed in the spectra during reduction are a 10-ns shift of the main peak centered at 65 ns to a longer delay time, and the development of a second major peak at ~45 ns. Thus, the node at ~45 ns in the untreated (oxidized) spectrum is transformed into the dominant peak in the reduced spectrum. During reoxidation, these changes were essentially reversed, as observed in the conventional Mössbauer spectra. It is unclear what caused the development of two peaks at 40 and 50 ns in the 5-min reoxidation spectrum, although it may relate to changes in sample "spectral" thickness caused by washing the excess reducing reagent out of the reaction cell with DI water.

3.2. Reaction Kinetics

To extract quantitative kinetic information from the synchrotron Mössbauer experiments, the signal intensity was integrated over a small delay-time window for each 30-s reaction-time step. As shown in Figure 3, the delay-time window was selected to provide the maximum contrast between the oxidized and reduced states and thus the most sensitive signal. The integrated signal intensity for each 30-s time step was then converted to Fe(II) mole fraction. The integrated signal in the delay-time window was assumed to be a linear combination of two signals, one each for the Fe(II) and Fe(III) components. To do this, a series of CONUSS©'a9 simulations was used to establish the relationship between Fe(II) content and delay-time window intensity for the range of Fe(II) contents observed. The actual delay-time window intensities were then normalized so that the end member (i.e., fully oxidized, maximum reduction) values matched the CONUSS©'a9-calculated values. Application of the regression equation for the calculated Fe(II)/intensity relationship to the normalized intensity data yielded the Fe(II) contents.

Kinetic plots of these experimental data (Fig. 6) show the reduction reaction reached completion in ~165 min. A faster overall reaction rate was observed during reoxidation, which reached completion in ~120 min. In part, this faster rate was due to the higher Cr(VI) concentration (i.e., 0.10 mol/L Cr(VI) vs. 0.05 mol/L $S_2O_4^{2-}$) that was used.

These two sets of data were also fit using the reactive diffusion model. As shown by the solid lines (Fig. 6), very reasonable fits of the reactive diffusion model to experimental data were obtained.

When the fixed and variable parameters used to achieve these fits (Table 2) are examined, three results stand out. First, the values for C_s are ~20-fold greater than the nominal bulk concentrations of the redox reagents. This result would be expected if the reagents adsorbed strongly to the solid surface, in effect increasing the reagent concentration at the reaction front. The affinity of anions (such as the redox reagents) for the positively charged basal surfaces of pyroaurite-like compounds is well known. Second, the values for D_1 and D_2 are roughly comparable (within a factor of 2) for the two reagents. This result also would be expected because both reagents are present as oxyanions with presumably similar diffusion properties. Third, the value of k_2 is nearly 300-fold smaller for the $S_2O_4^{2-}$ solution than for the Cr(VI) solution. This result was surprising, given the expected participation of the sulfoxyl free radical in the rate-determining step for the reduction reaction and the relatively fast kinetics typically observed for dithionite oxidation reactions (Creutz and Sutin, 1974).

The slower reaction rate constant for the reduction reaction could stem in part from a thermodynamic driving force that is in the "over-voltage" region for the reaction. At pH 5, the $S_2O_4^{2-}$ solution has a formal reduction potential of about −0.19 V for the half reaction to HSO_3^-. For the reoxidation reaction with Cr(VI), e.g.

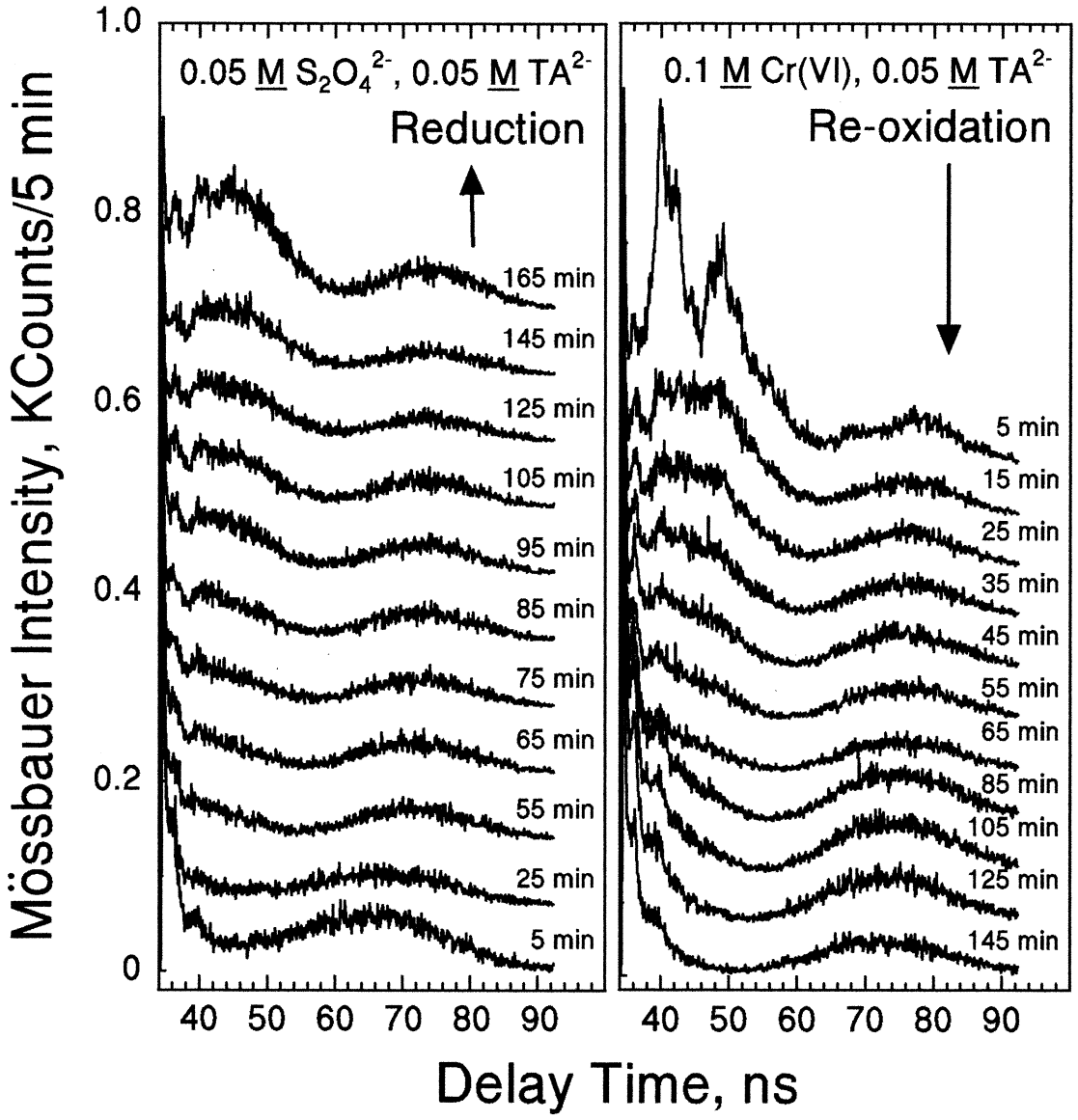

Fig. 5. Stacked plot showing changes in synchrotron Mössbauer spectra during reduction and subsequent reoxidation (February 1998 run).

$$HCrO_4^- + 4H^+ + 3e^- = Cr(OH)_3(s) + H_2O, \quad (4)$$

the standard potential is +1.35 V and the formal potential under the conditions of the experiment is about +0.77 V, equal to that of the aqueous Fe couple! Thus, the experimental results suggest that the reduction potential for structural Fe(III) in the pyroaurite-like compound is between −0.19 V and +0.77 V. Although we are not aware of thermodynamic data for this compound, such data are available for a similar layered-hydroxide compound, sulfate green rust $[Fe_4^{2+}Fe_2^{3+}(OH)_{12}SO_4{\cdot}3H_2O]$ (Hansen et al., 1994). Calculations for the solid-state reduction of sulfate green rust to $Fe(OH)_2(s)$ (assuming a final sulfate concentration equal to the TA concentration in our experiments) yield a formal potential of +0.02 V. This result, which is in the "over-voltage" region for the reduction reaction, is consistent with the observed reaction rate constant for the reduction being smaller than that for the reoxidation.

3.3. Comparison of Techniques

The main practical difference between the synchrotron and conventional approaches to ^{57}Fe Mössbauer spectroscopy is the relative speed with which synchrotron Mössbauer data can be collected. This speed stems from the very low noise inherent to the synchrotron technique, which stands in marked contrast to the conventional techniques where maximum noise levels are encountered. Both approaches allow collection of the full suite of Mössbauer parameters, such as center shift, quadrupole splitting, magnetic hyperfine field, and, when f-factors are known, Fe(II)/Fe(III) ratios. The synchrotron approach also allows direct determination of f-factors when the absorbing nuclei are present in a single type of site. The use of ^{57}Fe-enriched (92.4%) specimens allows the collection period to be as short as 30 s. With specimens having the natural abundance of ^{57}Fe (i.e., 2.1%), this period would be on the order of 20

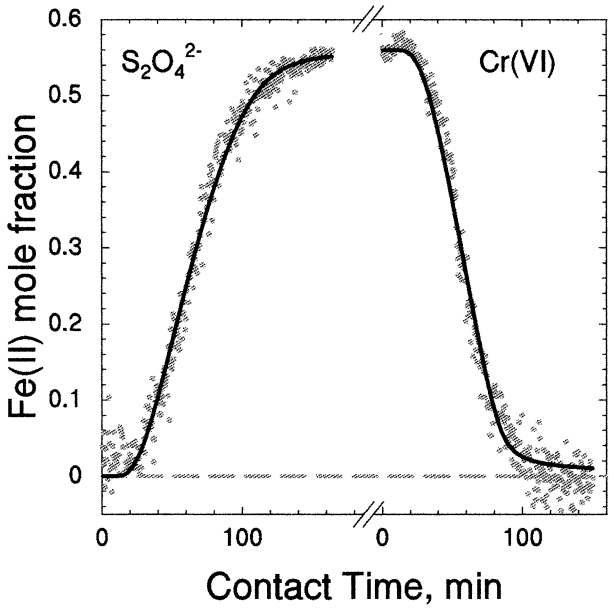

Fig. 6. Kinetic plot of time-integrated synchrotron Mössbauer signal intensity (normalized to measured Fe(II) mole fractions) obtained during reduction and reoxidation (February 1998 run). Solid line shows fit of reactive diffusion model to experimental data.

min. Under the temporal conditions (i.e., 30-s collection period) of our experiment, detection limits for ^{57}Fe(II), estimated conservatively as 3 times the standard deviation of the noise level, are ~8700 ppm or 6.4% of the ^{57}Fe present. With a 5-min collection period, these detection limits decrease to ~2300 ppm or 1.7% of the ^{57}Fe present.

Another synchrotron-based technique, XANES, has emerged in recent years for quantification of Fe(II)/Fe(III) ratios in minerals and similar systems (Bajt et al., 1994; Delaney et al., 1998; Dyar et al., 1998; Schmuki et al., 1998). Although not providing the complete description of the local Fe-site environment that is provided by the Mössbauer approach, the XANES approach is more easily adapted to microscopy and thus can be used much as an electron microprobe. Furthermore, it can be used with a larger suite of elements than Mössbauer spectroscopy. On the basis of the uncertainty in the measurement, which relies on the position of the preedge feature rather than its intensity (Bajt et al., 1994), detection limits with the XANES approach can be estimated at ~11% of the Fe. Where peak intensity is the relevant parameter, as with Mn XANES, detection limits as low as 2% of the total metal present have been estimated (Villinski et al., 2001). Although a typical high-quality XANES spectrum may take 15 to 60 min to collect, shorter periods can be used for kinetic experiments. For example, Mn K-edge XANES spectra were collected every 8 min by Villinski et al. (2001) for in situ monitoring of changes in Mn-oxide mineralogy during reaction with aqueous Fe(II). The developments of energy-dispersive EXAFS (Pellicer-Porres et al., 1998) and Quick-EXAFS (Lutzenkirchen-Hecht et al., 2001) allow data collection times on the order of 50 ms.

Relative to XANES spectroscopy, then, synchrotron ^{57}Fe Mössbauer spectroscopy thus offers the greatest advantage for experiments (1) *in aquo*, where the penetrating power of the 14.4-keV X-rays is ninefold greater than that of the 7.1-keV X-rays at the Fe K-edge, (2) where parameters in addition to Fe(II)/Fe(III) ratios are desired, and (3) where the highest accuracy in Fe(II)/Fe(III) ratio is required.

Table 2. Parameters from reactive diffusion model used to fit experimental synchrotron Mössbauer data (February 1998 run).

		Fitted Value	
Parameter	Units	Reduction by $S_2O_4^{2-}$	Re-oxidation by Cr(VI)
Fixed parameters			
b	μm	25.4	25.4
P	μm	250	250
r	μm	3000	3000
m	—	2	3
$Q_{Fe[un(0)]}$	mol	2.32E-05	1.30E-05
$Q_{Fe(\infty)}$	mol	1.30E-05	2.32E-05
$S_{(0)}$	μm^2	1[a]	1[a]
Variable parameters			
C_S	mol L^{-1}	1.41	2.39
D_1	$\mu m\ s^{-1}$	3.3E-02	2.9E-02
D_2	$\mu m\ s^{-1}$	5.4E + 02	1.1E + 03
k_2	L $mol^{-1}\ s^{-1}\ \mu m^{-2}$	5.9E + 04[a]	1.7E + 06[a]

[a] Reactive surface area not measured and arbitrarily set to 1 μm^2.

Acknowledgments—We gratefully acknowledge the design and fabrication skills of R. C. Nelson and M. R. Townsend at the Pacific Northwest National Laboratory (PNNL) and the helpful comments of two anonymous reviewers. This work was funded in part by the Laboratory Directed Research and Development program (PNNL) and in part by US DOE BES W-109-ENG-38 (ANL). The PNNL is operated for the U.S. Department of Energy by Battelle Memorial Institute under contract DE-AC06-76RL0 1830.

Associate editor: D. J. Vaughan

REFERENCES

Alp E. E., Sturhahn W., and Toellner T. (1995) Synchrotron Mössbauer spectroscopy of powder samples. *Nucl. Instr. Meth. Phys. Res. B* **97,** 526–529.

Alp E. E., Sinn H., Alatas A., Sturhahn W., Toellner T., Zhao J., Sutter J., Hu M., Shu D., and Shvydko Y. (2001a) Source and optics considerations for new generation high-resolution inelastic X-ray spectrometers. *Nucl. Instr. Meth. Phys. Res. A* **467,** 617–622.

Alp E. E., Sturhahn W., and Toellner T. S. (2001b) Lattice dynamics and inelastic nuclear resonant X-ray scattering. *J. Phys. Condens. Matter* **13,** 7645–7658.

Amonette J. E. (2003). Iron redox chemistry of clays and oxides: Environmental applications. In Electrochemical Properties of Clays, CMS Workshop Lectures, Vol. 10 (ed. A. Fitch), pp. 89–146. The Clay Minerals Society, Aurora, CA.

Amonette J. E. and Scott A. D. (1995) Oxidative Weathering of Trioctahedral Micas by Buffered H_2O_2 Solutions. In *Clays Controlling the Environment—Proceedings of the 10th International Clays Conference July 18–23, 1993, Adelaide, Australia* (eds. G. J. Churchman, R. W. Fitzpatrick, and R. A. Eggleton), pp. 355–361. CSIRO Publishing, Melbourne, Australia.

Bajt S., Sutton S. R., and Delaney J. S. (1994) X-ray microprobe analysis of iron oxidation states in silicates and oxides using X-ray absorption near edge structure (XANES). *Geochim. Cosmochim. Acta* **58,** 5209–5214.

Creutz C. and Sutin N. (1974) Kinetics of the reactions of sodium dithionite with dioxygen and hydrogen peroxide. *Inorg. Chem.* **13,** 2041–2043.

Danckwerts P. V. (1950) Absorption by simultaneous diffusion and chemical reaction. *Trans. Faraday Soc.* **46,** 300–304.

Danckwerts P. V. (1951) Absorption by simultaneous diffusion and chemical reaction into particles of various shapes and into falling drops. *Trans. Faraday Soc.* **47,** 1014–1023.

Delaney J. S., Dyar M. D., Sutton S. R., and Bajt S. (1998) Redox ratios with relevant resolution: Solving an old problem by using the synchrotron micro-XANES probe. *Geology* **26,** 139–142.

Drezdzon M. A. (1988) Synthesis of isopolymetalate-pillared hydrotalcite via organic-anion-pillared precursors. *Inorg. Chem.* **27,** 4628–4632.

Dyar M. D., Delaney J. S., Sutton S. R., and Schaefer M. W. (1998) Fe^{3+} distribution in oxidized olivine: A synchrotron micro-XANES study. *Am. Mineral.* **83,** 1361–1365.

Hansen H. C. B. and Koch C. B. (1998) Reduction of nitrate to ammonium by sulphate green rust: Activation energy and reaction mechanism. *Clay Miner.* **33,** 87–101.

Hansen H. C. B., Borggaard O. K., and Sorensen J. (1994) Evaluation of the free energy of formation of Fe(II)-Fe(III) hydroxide sulphate (green rust) and its reduction of nitrite. *Geochim. Cosmochim. Acta* **58,** 2599–2608.

Hansen H. C. B., Guldberg S., Erbs M., and Koch C. B. (2001) Kinetics of nitrate reduction by green rusts—Effects of interlayer anion and Fe(II): Fe(III) ratio. *Appl. Clay Sci.* **18,** 81–91.

Jost W. (1960) *Diffusion in Solids, Liquids, and Gases*. Academic Press.

Koch C. B. (1998) Structures and properties of anionic clay minerals. *Hyperfine Interactions* **117,** 131–157.

Kukkadapu R. K., Witkowski M. S., and Amonette J. E. (1997) Synthesis of a low-carbonate high-charge hydrotalcite-like compound at ambient pressure and atmosphere. *Chem. Mater.* **9,** 417–419.

Lasaga A. C. (1998) *Kinetic Theory in the Earth Sciences*. Princeton University Press.

Lutzenkirchen-Hecht D., Grundmann S., and Frahm R. (2001) Piezo-QEXAFS with fluorescence detection: Fast time-resolved investigations of dilute specimens. *J. Synchrotron Radiat.* **8,** 6–9.

Maxwell R. S., Kukkadapu R. K., Amonette J. E., and Cho H. M. (1999) ^2H solid-state NMR investigation of terephthalate anion dynamics in hydrotalcite-like compounds. *J. Phys. Chem. B* **103,** 5197–5203.

Miyata S. (1975) The synthesis of hydrotalcite-like compounds and their structure and physico-chemical properties. *Clays Clay Miner.* **23,** 369–375.

Miyata S., Kumura T., Shimada M. (1975) Composite metal hydroxides. U.S. Patent. 3879523. April 22, 1975.

Pellicer-Porres J., San Miguel A., and Fontaine A. (1998) High-focusing Bragg-crystal polychromator design for energy-dispersive X-ray absorption spectroscopy. *J. Synchrotron Radiat.* **5,** 1250–1257.

Raki L., Rancourt D. G., and Letellier C. (1995) Preparation, characterization, and Mössbauer spectroscopy of organic anion intercalated pyroaurite-like layered double hydroxides. *Chem. Mater.* **7,** 221–224.

Rancourt D. G. (1994) Mössbauer spectroscopy of minerals—I. Inadequacy of Lorentzian-line doublets in fitting spectra arising from quadrupole splitting distributions. *Phys. Chem. Miner.* **21,** 244–249.

Schmuki P., Virtanen S., Isaacs H. S., Ryan M. P., Davenport A. J., Böhni H., and Stenberg T. (1998) Electrochemical behavior of Cr_2O_3/Fe_2O_3 artificial passive films studied by in situ XANES. *J. Electrochem. Soc.* **145,** 791–801.

Scott A. D. and Amonette J. (1988) Role of iron in mica weathering. In *Iron in Soils and Clay Minerals* (eds. J. W. Stucki, B. A. Goodman, and U. Schwertmann), pp. 537–623. Reidel.

Sturhahn W. (1996) CONUSS, version 1.5. Fortran77 code written for UNIX operating system. Advanced Photon Source, Argonne National Laboratory, Argonne, Ill.

Sturhahn W., Alp E. E., Toellner T. S., Hession P., Hu M., and Sutter J. (1998) Introduction to nuclear resonant scattering with synchrotron radiation. *Hyperfine Interactions* **113,** 47–58.

Toellner T. S., Hu M. Y., Sturhahn W., Quast K., and Alp E. E. (1997) Inelastic nuclear resonant scattering with sub-meV energy resolution. *Appl. Phys. Lett.* **71,** 2112–2114.

Villinski J. E., O'Day P. A., Corley T. L., and Conklin M. H. (2001) In situ spectroscopic and solution analyses of the reductive dissolution of MnO_2 by Fe(II). *Environ. Sci. Technol.* **35,** 1157–1163.

Vucelic M., Jones W., and Moggridge G. D. (1997) Cation ordering in synthetic layered double hydroxides. *Clays Clay Miner.* **45,** 803–813.